ELSEVIER

Catalysis Today 43 (1998) 135–146

CATALYSIS TODAY

New selective Mo and NiMo HDS catalysts supported on Al_2O_3–MgO(x) mixed oxides

Tatiana Klimova, Dora Solís Casados, Jorge Ramírez*

UNICAT, Departamento de Ingeniería Química, Facultad de Química, UNAM, Cd. Universitaria, Coyoacán, Mexico D.F. (04510), Mexico

Abstract

In the search of selective hydrodesulfurization catalysts with low hydrogenating function, Mo and NiMo catalysts supported on Mg–Al mixed oxides with molar ratios x=MgO/(MgO+Al_2O_3)=0.0, 0.05, 0.25, 0.50, 0.75 and 1.0 were prepared by the sol–gel method. The synthesized solids were characterized by surface area, TGA, X-ray diffraction, temperature programmed reduction (TPR), DRS, FTIR and FT-Raman spectroscopy and high resolution electron microscopy (HREM). The catalysts were tested in the thiophene hydrodesulfurization reaction. The results indicate that even with the incorporation of small amounts of magnesia to the alumina support, the hydrogenation function of the catalyst is substantially reduced. The changes in the hydrodesulfurization and hydrogenation functions of the catalysts seem to be due to the formation of magnesium-molybdate and also due to the formation of a NiO–MgO solid solution which takes away the promoting effect of Ni. Therefore, in NiMo catalysts supported on magnesia containing supports, it is necessary to use Ni/(Ni+Mo) atomic ratios greater than 0.3 to recover the promotion effect lost by the interaction of NiO with magnesia. The results also indicate that only the catalysts with low magnesia content (x<0.25) show textural stability.

Keywords: Hydrodesulfurization; Hydrotreating catalysts; Aqueous impregnation; Magnesia; Nickel–molybdenum/magnesia; Alumina–magnesia

1. Introduction

The need of low sulfur reformulated gasoline requires to eliminate the sulfur compounds from all the streams which contribute to the gasoline pool. Most of the sulfur in a typical refinery gasoline pool comes from FCC naphthas which have a high olefin content and thus a high octane number. Elimination of the sulfur compounds from cracked naphthas is not a difficult task and, therefore, the severity of the required HDS process is not very high. However, during the HDS processing of cracked naphthas, significant saturation of the olefins present in the stream is also performed, leading to reduction of the octane. Therefore, the problem is that on one hand we need to perform deep hydrodesulfurization, but on the other, we need to diminish the loss of octane which occurs due to the simultaneous increase in the hydrogenation function of the catalyst. Clearly, this problem points out the necessity of new selective HDS catalysts, which can perform an adequate hydrodesulfurization but with low hydrogenation to avoid as much as possible the saturation of olefins, which contribute to the octane number in the product.

*Corresponding author. Fax:(525)622-5366; e-mail: jrs@servidor.unam.mx

0920-5861/98/$32.00
PII S0920-5861(98)00142-4

To accomplish the requirements of high HDS and low hydrogenation, catalysts with reduced acidity in the alumina support have been proposed [1,2]. However, other supports have also been proposed. For example, it has been reported in the literature [3] that for unpromoted Mo catalysts supported on different oxides the hydrogenating function varies according to: Al_2O_3>TiO_2>MgO>SiO_2. Also, the same authors report in the HDS of dibenzothiophene the lowest cyclohexylbenzene to biphenyl ratio for Mo catalysts supported on MgO, compared to those supported on Al_2O_3, TiO_2 and SiO_2. Magnesia supported hydrodesulfurization catalysts have been the object of only a few studies [1,3] and although magnesia supported sulfides are generally reported as less active for HDS than their alumina counterparts, they may be a good option for hydrodesulfurization of cracked naphthas with low olefins hydrogenation. Recently, it has been reported [4] that selectivity advantages, equal to a decrease of 10–40% in the olefin reduction at 80% HDS conversion, were achieved with CoMo catalysts supported on Mg–Al supports produced from the thermal decomposition of a crystalline hydrotalcite-like compound of formula $Mg_{4.5}Al_2(OH)_{13}$-$CO_{3.3}\cdot 5H_2O$. Some patents have also suggested the use of magnesia or mixtures of MgO with other refractory inorganic oxides as selective catalysts for hydrodesulfurization of cracked naphthas with low hydrogenation [2]. However, one of the disadvantages of MgO supported catalysts is that when in contact with moisture, the high surface area MgO (100–300 m^2/g) is transformed to low surface $Mg(OH)_2$ (10–30 m^2/g). It appears that even upon standing at ambient conditions MgO is converted to a mixture of $MgCO_3$ and $Mg(OH)_2$ [5]. Clearly, this process can also occur during the aqueous impregnation of the metal salts of the active-phase precursors. This process of loss of surface is a reversible one and the surface area can be again increased by calcination of the wet samples. Due to this complications, it has been proposed in the past the use of non-aqueous procedures for the impregnation of magnesia supported HDS catalysts [1]. Clearly, it should be interesting to find a way to stabilize magnesia-containing supports, to use them in selective hydrodesulfurization catalysts with low hydrogenation.

Thus, the object of this work will be to explore the possibility of stabilizing high surface areas in Mo and NiMo catalysts prepared by aqueous methods, by incorporating different amounts of Al_2O_3 to the MgO support using sol–gel procedures, and analyze the effect on the hydrodesulfurization and hydrogenation functions of the catalysts, measured in the thiophene HDS reaction, paying special attention to the hydrogenation conversion.

2. Experimental

2.1. Supports and catalysts preparation

The alumina–magnesia mixed oxides (Al–Mg(x)), with molar ratios x=MgO/(MgO+Al_2O_3)=0.0, 0.05, 0.25, 0.50, 0.75 and 1.0, were prepared using aluminum isopropoxide (Al(i-PrO)$_3$, Aldrich, 99%) and magnesium ethoxide ($Mg(OEt)_2$, Aldrich, 98%) as precursors and n-propyl alcohol as solvent. In each synthesis, 1.5 g of Al–Mg(x) sample were prepared according to the following procedure. The required amount of Al(i-PrO)$_3$ was dissolved in 300 ml of n-propanol (Aldrich, 99.5+%, HPLC grade) at room temperature under vigorous stirring. When the dissolution was over, the corresponding amount of $Mg(OEt)_2$ was added and the resulting solution was stirred for 2 h. Then, 50 ml of deionized water was added to the above solution to produce the precipitation of the metallic hydroxides. The precipitates were aged at room temperature with slow stirring for 24 h and then vacuum filtered. The resulting solids, after drying at 373 K for 24 h, were calcined in air for 24 h at 773 K.

Mo and NiMo/Al–Mg(x) catalysts were prepared by a standard incipient wetness technique. The calcined supports were impregnated successively with an aqueous solution of ammonium heptamolybdate and nickel nitrate according to the required Mo and Ni loading: 2.8 at/nm^2 of molybdenum and a nickel content corresponding to an atomic ratio r=0.3, where r=Ni/(Ni+Mo). NiMo catalysts with r=0.4 and 0.6 were also prepared for the supports with x=0.05 and 1.0. After each impregnation, the solids were dried at 373 K (12 h) and finally calcined at 773 K (4 h). Prior to the catalytic activity tests the catalysts were sulfided in situ in a stream of 15% volume of H_2S in H_2 during 4 h at 673 K.

2.2. Catalytic activities

Catalytic activities in the thiophene hydrodesulfurization reaction were determined at steady state conditions, after a 12 h stabilization period using a flow microreactor operating at atmospheric pressure. In all the experiments the feed rate of TH, F(TH), was 1.53 mmol h^{-1} and the feed rate of hydrogen was 50 mmol h^{-1}. For the Mo series catalysts, the catalyst charge, W, was 0.1 g, and 0.05 g for NiMo catalysts. The thiophene conversion at a fixed value of W/F(TH) was sequentially determined at four temperatures from 533 to 623 K in steps of 30 K. To evaluate the hydrogenation (HYD) function, also the conversion to butane, defined as moles of butane in the product per mole of thiophene in the feed, was followed.

2.3. Catalyst characterization

The samples were characterized by nitrogen physisorption measurements, FTIR and FT-Raman spectroscopy, thermogravimetry (TG), X-ray powder diffraction (XRD), UV–VIS diffuse reflectance spectroscopy (DRS), temperature-programmed reduction (TPR) and high resolution electron microscopy (HREM). All the characterizations were made with the calcined samples, except the thermal analysis of the supports in which the uncalcined samples were used as starting materials. The surface area and pore characteristics of supports and catalysts (in their oxide state) were obtained using a Micromeritics ASAP 2000 system. Prior to the physisorption measurements, all samples were outgassed for 3 h at 523 K. In general, the errors found in repeated measurements of surface area determinations were within 2–3% of the total surface area. FTIR measurements were performed with a Nicolet 510 spectrometer using KBr pressed disks. Dehydration of the samples was achieved by heating, under vacuum, the pressed disks at 523 K for 1 h. The IR spectra were recorded at room temperature, with 300 scans and 4 cm^{-1} resolution. The laser Raman spectra were recorded in the 400–4000 cm^{-1} range on a Nicolet 950 FT spectrometer. A Nd-YAG laser was used as the excitation source with a slit width setting of 4 cm^{-1}. Signal detection was achieved with an InGaAs detector. All the samples were diluted in 50 times with KBr. Thermogravimetric analysis was carried out in a Dupont 2000 system, under a nitrogen flow of 100 ml min^{-1} and a heating rate of 10 K min^{-1}. X-ray diffraction patterns were recorded in the range $3^\circ \leq 2\Theta \leq 80^\circ$ in a Philips PW 1050/25 diffractometer, using Fe-filtered CuKα radiation (λ=1.5418 Å) and a goniometer speed of $2^\circ(2\Theta)$ min^{-1}. UV–VIS–NIR electronic spectra of the samples were recorded in the wavelength range 250–2500 nm using a Cary-5E spectrophotometer with a diffuse reflectance attachment. Al–Mg(X) supports were used as a reference. The value of the Schuster-Kubelka-Munck remission function was determined. Temperature-programmed reduction experiments were performed in an ISRI-100 catalyst characterization system, with catharometric detection of hydrogen consumption. In these experiments, 125 mg samples were reduced in a stream of 70% H_2/Ar gas mixture (25 ml min^{-1}) from 293 to 1273 K at a heating rate of 10 K min^{-1}. Prior to each measurement the sample was pretreated in a stream of N_2 at 773 K for 2 h. High resolution transmission electron microscopy studies were performed using a Jeol 2010 microscope (resolving power 1.9 Å). The solids were ultrasonically dispersed in heptane and the suspension was collected on carbon-coated copper grids.

3. Results and discussion

3.1. Catalytic activity

Conversion of thiophene and the production of butane on the Mo/Al–Mg(x) catalysts, as a function of the magnesia content, in the thiophene hydrodesulfurization reaction, are presented in Figs. 1 and 2. Here, one can see that the catalysts supported on alumina have the highest activity and that only a small activity drop, which is practically independent of the MgO loading, is obtained by the incorporation of different amounts of MgO into the support formulation. However, the hydrogenation of butenes to butane is substantially reduced when small amounts of MgO are incorporated to the alumina. Further increase in the MgO content of the catalyst do not produce further important changes in its hydrodesulfurization and hydrogenation activity. In contrast, the nickel promoted catalysts with a Ni/(Ni+Mo) ratio of 0.3, Figs. 3 and 4, present a continuous and substantial drop in HDS activity with magnesia loading. In fact,

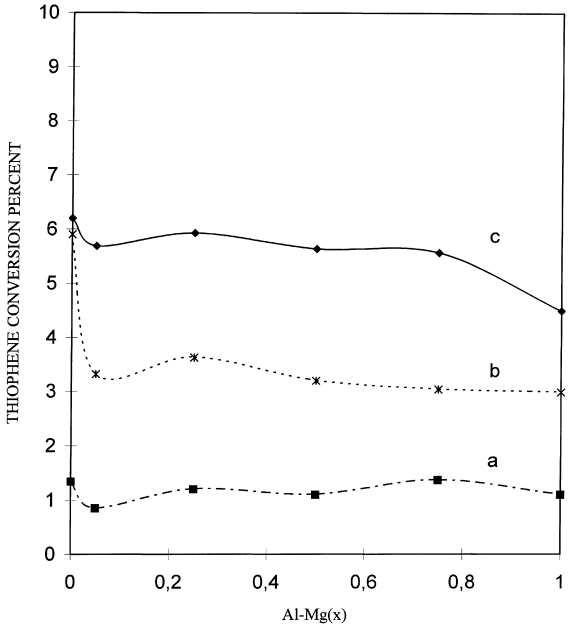

Fig. 1. Thiophene conversion (%) in Mo/Al–Mg(x) catalysts: (a) 533 K, (b) 593 K and (c) 623 K.

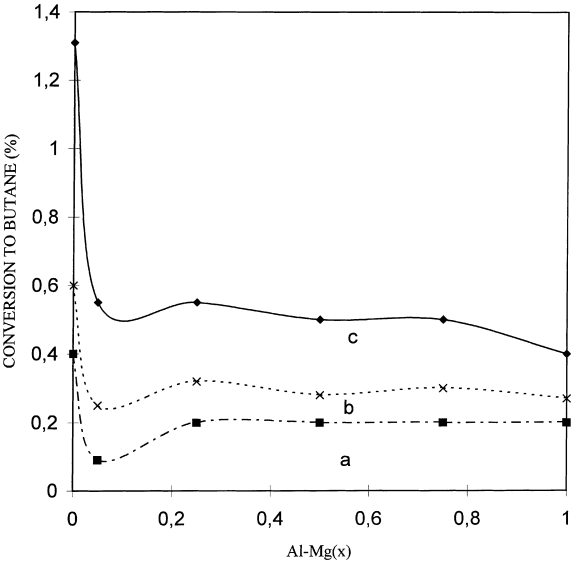

Fig. 2. Conversion to butane (%) in Mo/Al–Mg(x) catalysts: (a) 533 K, (b) 593 K and (c) 623 K.

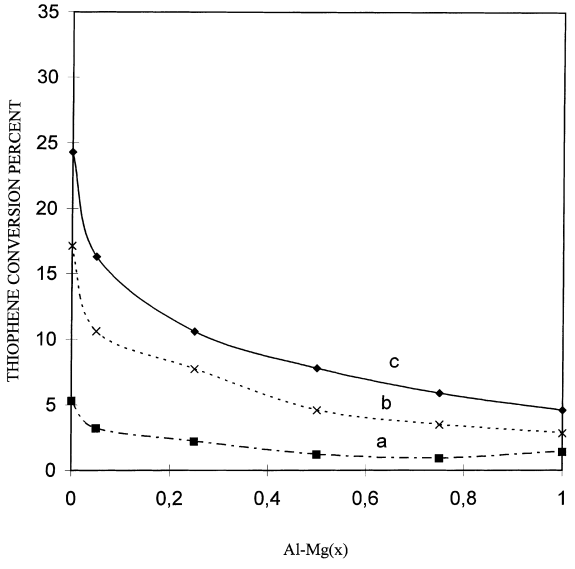

Fig. 3. Thiophene conversion (%) in NiMo/Al–Mg(x) catalysts: (a) 533 K, (b) 593 K and (c) 623 K.

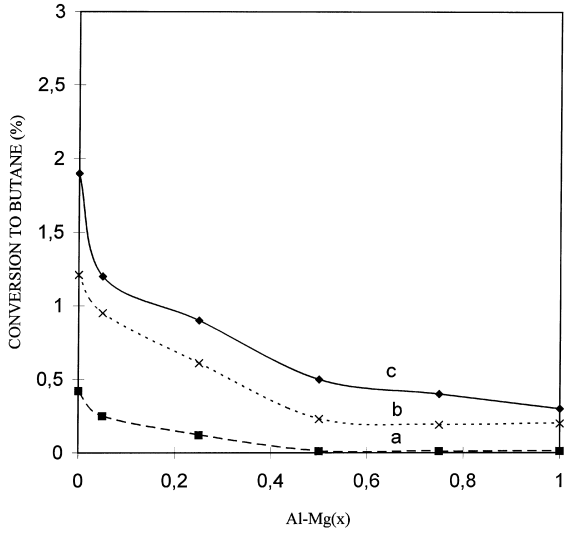

Fig. 4. Conversion to butane (%) in NiMo/Al–Mg(x) catalysts: (a) 533 K, (b) 593 K and (c) 623 K.

the activity drop is so important with magnesia loading that the pure magnesia supported catalyst shows a thiophene conversion which is similar to that of the unpromoted Mo/Al–Mg(1.0) catalyst. This result indicates the loss of the Ni promotion effect as the magnesia loading in the catalyst increases. These results could be rationalized by considering the possibility of formation of a NiO–MgO solid solution

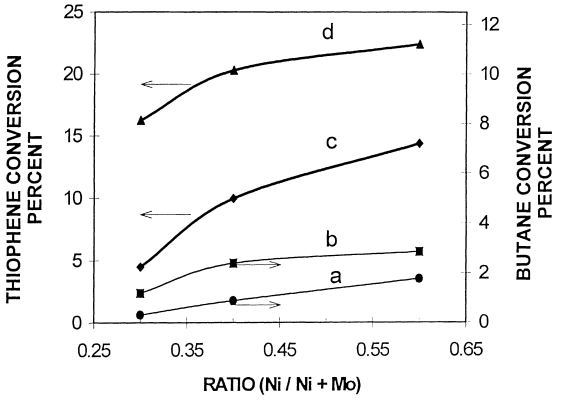

Fig. 5. Conversion to butane (%) in NiMo/Al–Mg(x) catalysts with r =0.3, 0.4 and 0.6, when (a) x=1.0 and (b) 0.05; and thiophene conversion (%): (c) x=1.0 and (d) 0.05.

which consumes most of the nickel in the catalysts with Ni/(Ni+Mo)=0.3, and also to the formation of a small amount of magnesium molybdate. In line with this suggestion, an increase in the Ni/(Ni+Mo) ratio in the catalysts leads to a marked recovery of the HDS activity (Fig. 5). This activity recovery is also evident for the NiMo/Al–Mg(0.05) catalyst.

Clearly, the changes in catalytic activity and conversion to butane observed in the Mo and NiMo catalysts with the amount of magnesia in the support must be related, at least in part, to the textural and structural characteristics of the support and to its interaction with the Mo and Ni phases.

3.2. Supports and catalysts characterization

The textural properties of the different supports and catalysts compositions are presented in Table 1. From this table, it is possible to see that the fresh-prepared supports can be obtained with high specific surface areas. Lower surface areas are obtained only when the concentration of MgO in the support is beyond x=0.50. This loss of surface area is accompanied by an increase in pore diameter. The successive aqueous impregnation of Mo and Ni to the Al–Mg(x) support induces the formation of low surface area $Mg(OH)_2$ but during drying and calcination MgO is formed again and, as the results from Table 1 show, the surface area is restored and in some cases increased. During this process the pore diameter and the pore volume are decreased. It is only the pure MgO supported catalysts which show an erratic behavior. In this case, probably due to the extent of the solubilization–recrystalization process of magnesia, after the Mo and Ni impregnation, the surface area is increased as also the pore diameter and the pore volume indicating a massive textural change leading to solids with bigger pores with thin walls.

It is important to point out that the magnesia-rich catalysts (x>0.25) do not show textural stability and they tend to lose surface area with time, when they are kept at ambient conditions.

According to the XRD results (Figs. 6 and 7), it appears that the incorporation of magnesia to the pure alumina support renders the alumina more amorphous since the two main peaks (I/I_0=100 and 80%) corresponding to interplanar distances of 1.4 and 1.98 Å, which appear clearly in the pure alumina support, almost disappear at magnesia contents beyond x=0.25 and instead, reflections corresponding to MgO appear in the diffractogram. It seems that the magnesium–aluminum oxide with spinel structure is not formed at the conditions of our experiment since

Table 1
Fresh-prepared supports, Mo and NiMo catalysts

x	Al–Mg(x) oxides			Mo/Al–Mg(x) catalysts			NiMo/Al–Mg(x) catalysts		
	S_{BET} (m^2/g)	dp [a] (Å)	V (cm^3/g)	S_{BET} (m^2/g)	dp [a] (Å)	V (cm^3/g)	S_{BET} (m^2/g)	dp [a] (Å)	V (cm^3/g)
0.00	224	79	0.45	199	70	0.35	187	71	0.33
0.05	238	58	0.35	261	42	0.27	246	44	0.25
0.25	226	58	0.33	210	43	0.23	192	44	0.21
0.50	212	63	0.33	220	35	0.19	186	41	0.19
0.75	193	93	0.44	224	34	0.19	192	45	0.22
1.00	130	104	0.34	329	69	0.56	154	150	0.58

[a] dp - average pore diameter.

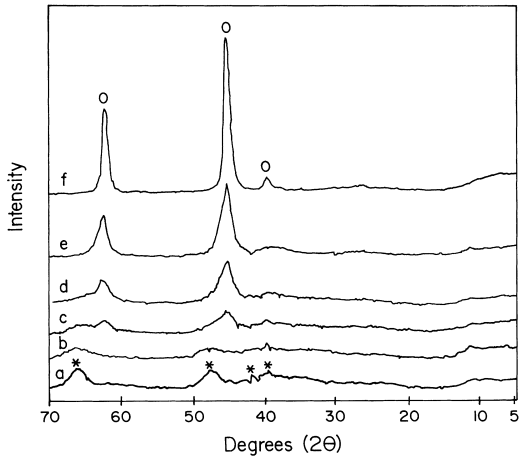

Fig. 6. X-ray diffraction of Al–Mg(x) oxides: (a) x=0.0, (b) x=0.05, (c) x=0.25, (d) x=0.50, (e) x=0.75 and (f) x=1.0.

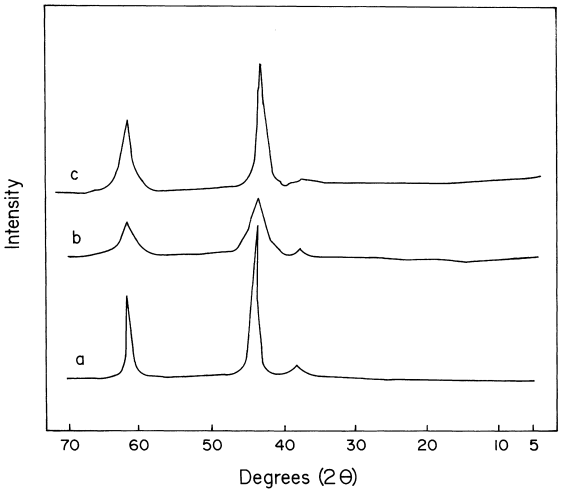

Fig. 7. X-ray diffraction of (a) Al–Mg(1.0), (b) Mo/Al–Mg(1.0) and (c) NiMo/Al–Mg(1.0) catalysts.

the main reflection for the spinel type oxide should appear at 2Θ=36.80 and is not evident in the diffractogram of any of the samples. An interesting fact observed when comparing the diffractograms of supports with those of the unpromoted and nickel-promoted samples is that the incorporation of molybdenum to the support induces a loss in the crystallinity of the magnesia peaks which now appear more broad and less intense. In contrast, the subsequent incorporation of Ni to the catalyst produces a recovery of the magnesia phase crystallinity. These changes indicate that some interaction between the Mo and Ni oxides with the support is taking place. In fact, the existence of a MgO–NiO solid solution has been well documented [6].

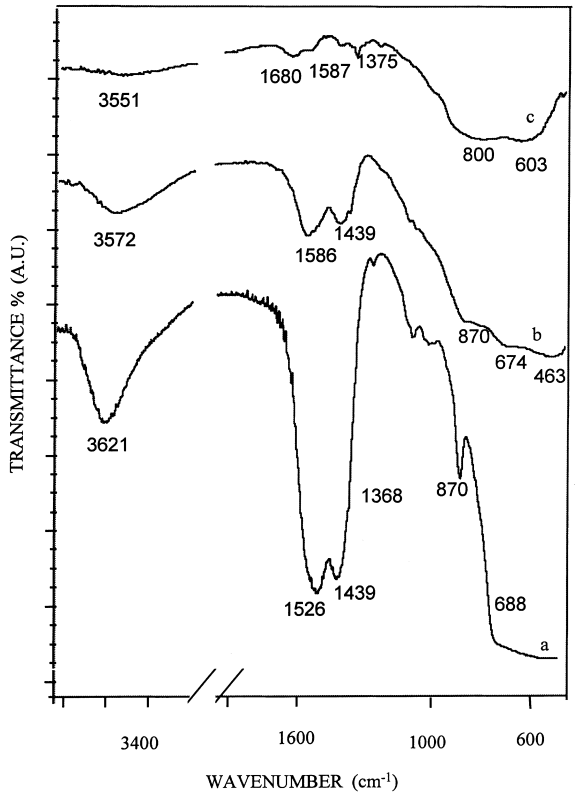

Fig. 8. FTIR spectra of the Al–Mg(x) samples: (a) x=1.0, (b) x=0.50 and (c) x=0.0.

Fig. 8 shows the FTIR spectra of the Al–Mg (x=0, 0.5, 1.0) supports. In the OH's region, the shift observed in the broad band due to the free hydroxyls of the supports, shows a gradual change in the nature of the OH groups from pure magnesia to pure alumina. The spectra also show, in agreement with literature data [5], that under ambient conditions the support contains carbonates and that their amount increases with magnesium content. The observed bands correspond to ionic CO_3^{2-} (1439 cm^{-1}), physisorbed CO_2 (1526 cm^{-1}) and monodentate $-O-CO_2^-$ (1375 cm^{-1}), the latter appearing only as a shoulder

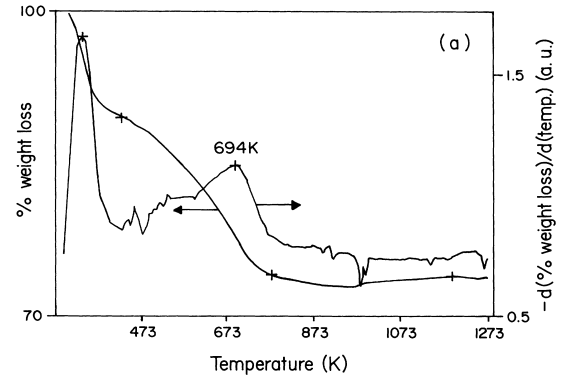

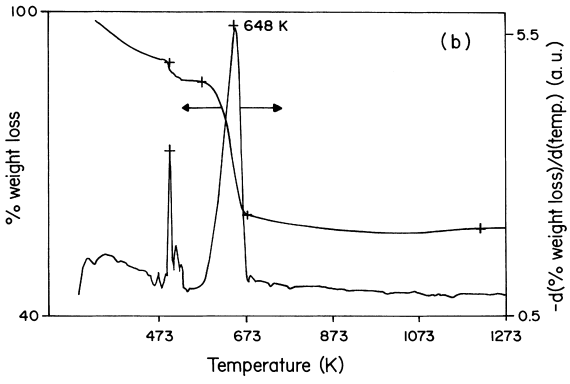

Fig. 9. Thermogravimetric analysis of Al–Mg(x) samples: (a) x=0.0, (b) x=1.0.

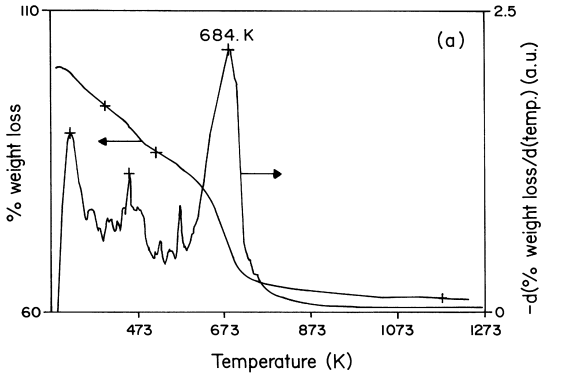

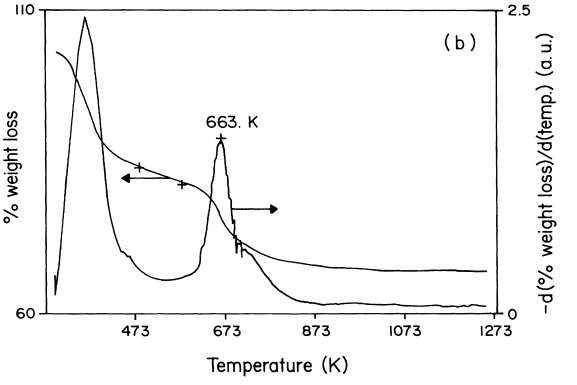

Fig. 10. Thermogravimetric analysis of Al–Mg(x) samples: (a) x=0.50, (b) mechanical mixture x=0.50.

in the pure magnesia sample. In the fundamental region at 500–900 cm^{-1} the pure alumina sample shows two broad bands assigned to vibrations Al–O of tetrahedral (800 cm^{-1}) and octahedral (603 cm^{-1}) aluminum. In the Al–Mg(0.5) mixed oxide the above bands are not so clear but the appearance of a new band at 673 cm^{-1} hints the existence of aluminum with intermediate coordination between tetrahedral and octahedral. This result is in line with the XRD results which show a loss of crystallinity of the alumina with the incorporation of small amounts of magnesia to the support.

The interaction between alumina and magnesia in the supports is also confirmed by the thermal analysis results (Figs. 9 and 10) which show that the loss of weight assigned to the dehydroxylation of the dried support samples occurs at different temperatures in the Al–Mg(0.5), Al–Mg(1.0) and Al–Mg(0) samples (T_{max} =684, 648 and 694 K, respectively). To corroborate this even further, the thermogram of a mechanical mixture, Al_2O_3–MgO, with a composition equivalent to x=0.5, also shown in Fig. 10, reveals a main peak at 662 K assigned to the loss of hydroxyl groups in magnesia, and a shoulder at about 713 K assigned to the dehydroxylation of alumina. These peaks are clearly different from those obtained with the mixed oxide. It appears then from the above results that the mixed supports are composed mainly of the corresponding mixed oxide and some small amounts of the pure Al_2O_3 and MgO phases.

Regarding the Mo and Ni phases the XRD results indicate, at this scale of measuring, good dispersion of the metallic phases since no evidence of diffraction lines from either Ni or Mo oxide phases were evident. However, according to the TPR results of the unpromoted catalyst samples (Fig. 11), different species of Mo are present on the catalyst surface and their population changes with the magnesia content in

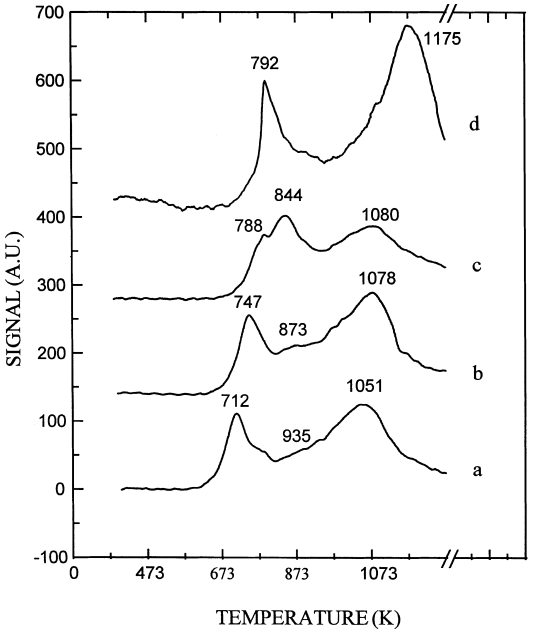

Fig. 11. TPR of Mo/Al–Mg(x) catalyst: (a) x=0.0, (b) x=0.05, (c) x=0.25 and (d) x=1.0.

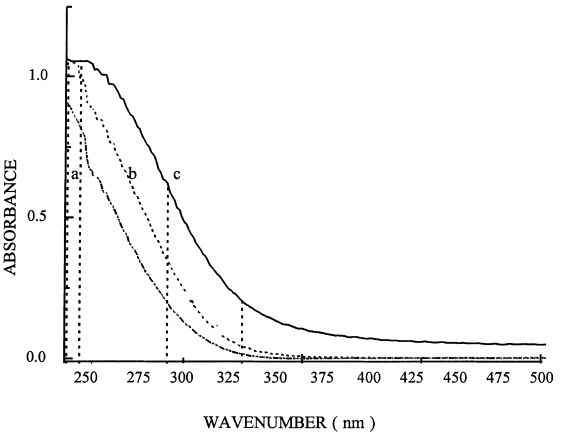

Fig. 12. UV–VIS spectra of Mo/Al–Mg(x) catalysts: (a) x=1.0, (b) x=0.5 and (c) x=0.0.

the catalyst. The assignation of the TPR hydrogen consumption peaks has been made on the basis of previous literature reports on Mo based catalysts supported on alumina [7,8] and magnesia [9]. For the pure alumina supported catalyst, two reduction peaks with maxima at 712 and 1051 K, which correspond to the presence of octahedral and tetrahedral molybdenum species, respectively, are clearly evident. Also, in the temperature range 773–923 K the reduction of polymeric Mo species and MoO_3 is evident by the appearance of shoulders in the peaks of octahedral and tetrahedral Mo. As magnesia is incorporated into the support, Mo/Al–Mg (0.05) sample, the zone of intermediate reduction temperature begins to grow and also, an increase in the consumption of hydrogen is observed at high temperature (1173–1273 K). The incorporation of more magnesia to the support (Mo/Al–Mg (0.25) sample) definitely changes the distribution of the Mo species and, in this case, the peak corresponding to species of octahedral Mo, which in alumina appeared at 712 K, appears only as a shoulder at 788 K. At the same time, the peak of polymeric Mo species becomes clearly defined presenting a maximum at 844 K. Since the contribution of the high temperature shoulder also becomes more important with the magnesium content, it appears that in addition to the population of new polymeric species in interaction with the support, more tetrahedral Mo species, which reduce at high temperature, are produced at the expense of octahedral Mo and possibly of highly dispersed MoO_3 species. This grow in tetrahedral species is also evidenced by the displacement of the high temperature maximum from 1051 K in alumina to about 1175 K in the pure magnesia-supported catalyst. These observations are well in line with the DRS results (Fig. 12), which show that as magnesia is incorporated to the catalyst support the absorption edge shifts to lower wavenumbers indicating, based on the assignations of Mo species reported previously in the literature for alumina [10–12] and magnesia [9] supported Mo catalysts, a diminishing of octahedral Mo species in favor of tetrahedral ones.

The observed changes in the nature of the Mo species with magnesium content are also evidenced by the FT-Raman results of unpromoted Mo catalysts (Fig. 13), which show, in the alumina supported catalyst, vibrations corresponding to the presence of MoO_3 (band at 820 cm^{-1}) [13–15], and that as the magnesia content is increased this band tends to disappear. This observation can be rationalized by considering either a higher dispersion of the Mo species on the magnesia containing catalysts or the formation of a new phase of molybdenum and magnesium, possibly magnesium molybdate. In line with

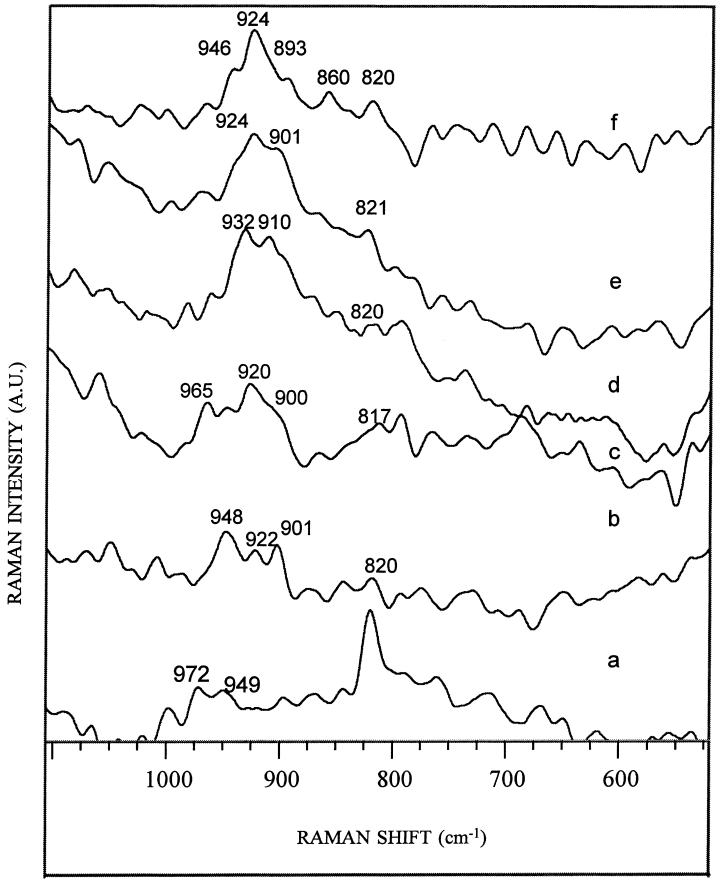

Fig. 13. Raman spectra of Mo/Al–Mg(x) catalysts: a) x=0.0, (b) x=0.05, (c) x=0.25, (d) x=0.50, (e) x=0.75 and (f) x=1.0.

this, the band corresponding to M=O vibrations of molybdenum oxo species in interaction with the support, and which have been reported at about 950 and 915 cm^{-1} for Mo supported on alumina and magnesia, respectively [3], shifts from 949 cm^{-1} in the pure alumina supported catalyst to 924 cm^{-1} in the pure magnesia supported catalyst. This band has been assigned to species MoO_4^{2-} [15], and in this case can be due to the formation of $MgMoO_4$. In fact, surface molybdenum species supported on magnesia have been reported as responsible for a Raman band at 915 cm^{-1} [3] and 855, 907, 967 and 1094 cm^{-1} [16]. In the latter reference the authors indicate that the type of Mo surface species that produce such richness in band structure has not yet been clearly elucidated. The difference in bands observed in the above references might be due to the fact that in reference [3] the spectra were taken at ambient conditions where some hydration of the samples is expected and in reference [16] the spectra were taken under vacuum after heat treatment. Therefore our results, which were also taken at ambient conditions, should be closer to those in reference [3]. Nevertheless, our spectra show a high degree of complexity in the band structure.

The electron microscopy results of the catalysts in the sulfided state (Figs. 14 and 15) show the typical fringes due to MoS_2 crystallites with 6.2 Å interplanar distances. In the alumina supported catalyst MoS_2 crystallites with average lengths of about 40 Å and stacking of about one to three layers are observed. In contrast, on the magnesia containing catalysts and specially on the pure magnesia supported catalyst,

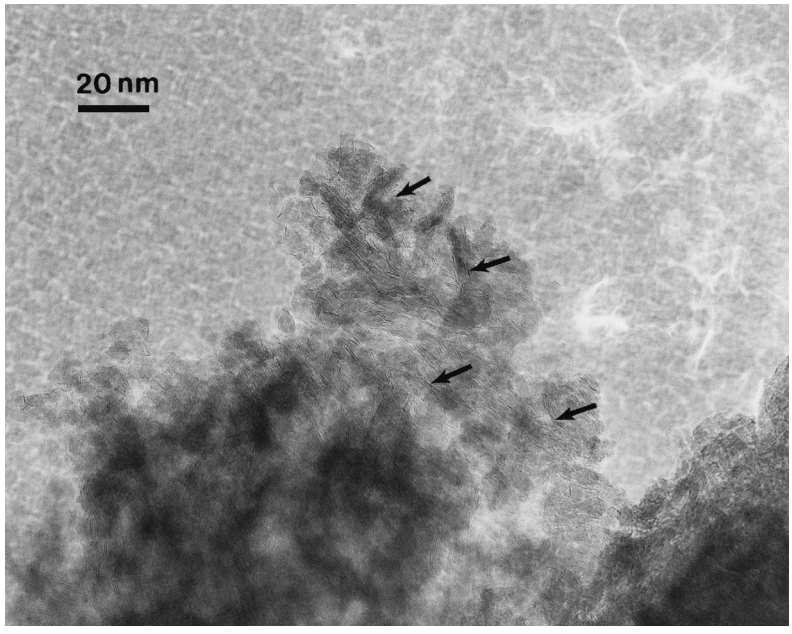

Fig. 14. HREM micrograph of NiMo/Al–Mg(0.0) catalyst.

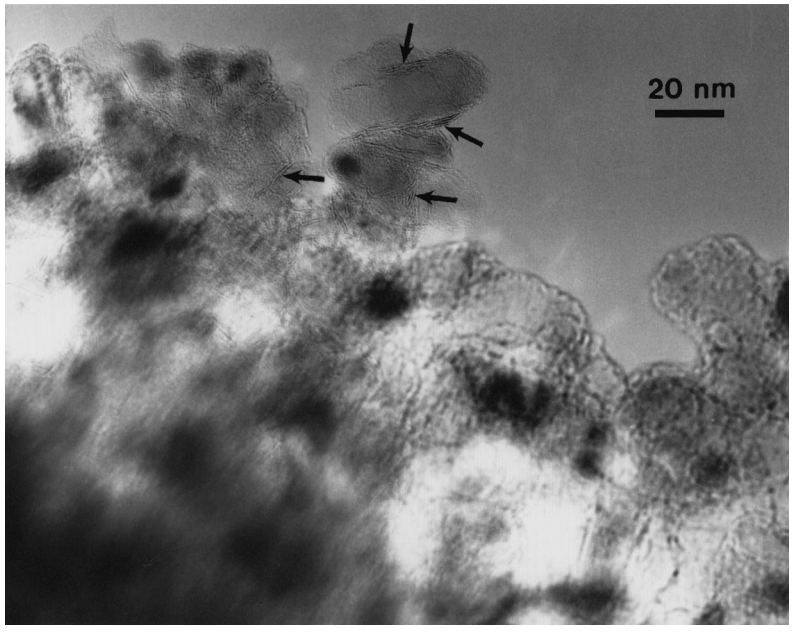

Fig. 15. HREM micrograph of NiMo/Al–Mg(1.0) catalyst.

longer crystallites are observed. This longer crystallites are specially observed on the outer surface of magnesia particles. This observations can be rationalized, according to the characterization results from the other techniques, by considering that the interaction between the magnesia support and the molybde-

num oxidic phases in the catalyst precursors leads under calcination to the formation of magnesium molybdate surface layers. These layers of magnesium molybdate lead, under sulfidation, to the observed continuous layers of MoS_2 around the magnesia particles. The fact that these MoS_2 layers are observed in both the promoted and unpromoted catalysts, and that they appear not only in the pure magnesia supported catalyst, but in almost all the magnesia containing catalysts except in those with a very low magnesia content (x=0.5, 0.25), supports even further the idea that a sulfidable molybdenum–magnesium phase is formed and that a substantial part of the Ni promoter is lost in the magnesia structure by forming a solid solution since it is well known that Ni takes positions at the edges of the MoS_2 crystallites impeding their lateral growth and leading therefore to smaller size MoS_2 crystallites. Moreover, unpromoted MoS_2 crystallites in other supports like Al_2O_3, TiO_2, ZrO_2 [17,18] have sizes between 25 and 40 Å whereas in the magnesia supported catalysts crystallites of about 80 Å are present.

Based on the above characterizations the catalytic activity trends for the unpromoted and promoted catalysts can be rationalized as follows:

For the unpromoted Mo catalysts the small drop in activity with magnesia content can be explained, according to the TPR result, in relation to the formation of less reducible, and possible less sulfidable, Mo species. These Mo species will be in a strong interaction, and in some cases will form a different compound with the magnesia support.

In the case of the Ni promoted catalysts the characterization results indicate the formation of a NiO–MgO solid solution which leads, as the magnesia content in the catalyst is increased, to a greater deficiency in the promotion by Ni of the Mo active species.

The decrease in the hydrogenation/hydrodesulfurization ratio with the magnesia content in the catalyst can be rationalized in terms of the change in the size of the MoS_2 crystallites. Our HREM results indicate an increase in the size of the MoS_2 crystallites with magnesia content which would lead to an increased proportion of edge versus corner sites in the MoS_2 crystallites. It would appear then that the hydrogenation sites could be related to corner sites. In line with this suggestion, previous results have indicated, for W catalysts, which behave in a similar way to those based in Mo, that the hydrogenation activity is related to the population of metal-oxygen (M=O) terminal bonds, rather than to the metal-oxygen-metal (M-O-M) bridge bonds in the oxidic precursors [19]. One may infer that the terminal bonds in the oxidic precursors would be related to the corner sites and that the bridge bonds would be related to the edge sites in the sulfided MoS_2 crystallites. It would appear then that the decrease in the Mo corner sites, which results from the growing of the MoS_2 crystallites as the magnesia content is increased, leads to a decrease in the hydrogenation activity.

4. Conclusions

According to the above results, the following conclusions can be stated:

1. The use of Al_2O_3–MgO mixed oxides allows to obtain magnesia-containing catalytic supports with surface areas which are maintained during aqueous impregnation of the active phases, however, long range textural stability is only achieved at low magnesia contents (x=0.05, 0.25).
2. The use of Al–Mg mixed oxides allows, in the case of Mo/Al–Mg(x) catalysts, a substantial decrease in hydrogenation with only a small drop in hydrodesulfurization activity.
3. In the case of NiMo/Al–Mg(x) catalysts, a substantial drop in both, hydrodesulfurization and hydrogenation activities with magnesia content seems to be related to the formation of a NiO–MgO solid solution which at high magnesia content (x=1.0) practically cancels the Ni promotion effect.
4. Greater catalytic activities in NiMo-magnesia-containing catalysts can be achieved by increasing the Ni/(Ni+Mo) atomic ratio in the catalyst beyond 0.3.
5. The FT-Raman and HREM results indicate that in magnesia supported catalysts the Mo oxidic species in interaction with the support are different from those in alumina supported ones and lead, under sulfidation to longer MoS_2 crystallites (≈80Å), which seem to be the result of $MgMoO_4$ sulfidation.

Acknowledgements

Financial support for this work by DGAPA-UNAM, CONACyT, IMP FIES program and PEMEX-Refinación is gratefully acknowledged. We would like to thank Ivan Puente-Lee for obtaining the HREM micrographs and Perla Castillo for her help with the TPR measurements.

References

[1] E. Hillerová, Z. Vit, M. Zdrazil, Appl. Catal. 118 (1994) 111.
[2] R.J. Bertolacini, T.A. Sue-A-Quan, U.S. Patent 4, 140, 626.
[3] H. Shimada, T. Sato, Y. Yoshimura, J. Hiraishi, A. Nishijima, J. Catal. 110 (1988) 275.
[4] D.E. Sherwood, Jr., E.P. Dai., Proceedings of 14th North American Meeting of the Catalysis Society, 11–16 June, 1995, p. T-192.
[5] S.E. Wanke, R.M.J. Fiedorow, in: K.K. Unger, J. Rouquerol, K.S.W. Sing, H. Kral (Eds.), Characterization of porous solids (Studies in Surface Science and Catalysis). vol. 39, Proc. IUPAC Symp. (COPS II) Bad Soden, 1987, Elsevier Amsterdam, The Netherlands, 1988, p. 601.
[6] F. Arena, B.A. Horrel, D.L. Cocke, A. Parmaliana, N. Giordano, J. Catal. 132 (1991) 58.
[7] R. López Cordero, F.J. Gil Llambias, A. López Agudo, Appl. Catal. 74 (1991) 125.
[8] R. López Cordero, J. Lázaro, J.L.G. Fierro, A. López Agudo, in: F. Cossio, O. Bermudez, G. del Angel, R. Gómez (Eds.), Actas XI Simposio Iberoamericano de Catálisis, IMP-SIC, Junio 1988, México D.F., pp. 563–570; and references therein.
[9] J.M.M. Llorente, V. Rives, P. Malet, F.J. Gil-Llambías, J. Catal. 135 (1992) 1.
[10] J.H. Ashley, P.C.H. Mitchel, J. Chem. Soc. A (1968) 2821.
[11] N. Giordano, J.C.H. Bart, A. Vaghi, A. Castellan, G. Martinotti, J. Catal. 36 (1975) 81.
[12] H. Praliaud, J. Less Common Metals 54 (1977) 387.
[13] L. Wang, W.K. Hall, J. Catal. 83 (1983) 242.
[14] F.R. Brown, L.E. Makovsky, K.H. Rhee, J. Catal. 50 (1977) 162.
[15] G.E. Vrieland, C.B. Murchison, Appl. Catal. A: General 134 (1996) 101.
[16] J.M. Stencel, L.E. Makovsky, T.A. Sarkus, J. de Vries, R. Thomas, J.A. Moulijn, J. Catal. 90 (1984) 314.
[17] J. Ramírez, S. Fuentes, G. Díaz, M. Vrinat, M. Breysse, M. Lacroix, Appl. Catal. 52 (1989) 211.
[18] M. Vrinat, M. Breysse, C. Geantet, J. Ramírez, F. Massoth, Catal. Lett. 26 (1994) 25.
[19] T. Halachev, P. Atanasova, A. Lopez Agudo, M.G. Arias, J. Ramirez, Appl. Catal. A: General 136 (1996) 161.